

Supporting Information

Facile, Rapid, and Large-Area Periodic Patterning of Semiconductor Substrates with Sub-Micron Inorganic Structures

Thomas J. Kempa,¹ D. Kwabena Bediako,¹ Evan C. Jones,¹
Charles M. Lieber^{1,2*} and Daniel G. Nocera^{1*}

¹ *Department of Chemistry and Chemical Biology, Harvard University, Cambridge, MA 02138.*

² *School of Engineering and Applied Sciences, Harvard University, Cambridge, MA 02138.*

e-mail: dnocera@fas.harvard.edu, cml@cmliris.harvard.edu

<i>Index</i>	<i>Page</i>
Methods	S2
Fig. S1 Electrochemical set-up of RIPPLE technique	S4
Fig. S2 Geometry and composition of patterned concentric rings	S5
Fig. S3 Topographical analysis of patterned Ge rings by AFM	S6
Fig. S4 Pattern morphology with CV performed in Na ₂ SO ₄	S8
Fig. S5 Single patterning experiment at two scan rates	S9
Fig. S6 Patterning and anodization of Co	S10
Fig. S7 CVs of patterned CoP _i	S11
Fig. S8 Stability of patterned CoP _i catalyst	S12

METHODS

Substrate Preparation. Si <111> p-type doped substrates (Prime Grade 3-5 Ω cm, Nova Electronic Materials) were cleaned using a UV/ozone system at 300 °C for 5 min. The substrates were etched for 10 s in buffered hydrogen fluoride and then inserted into a home-built chemical vapor deposition (CVD) reactor, which was evacuated to a base pressure of 5.4 mTorr. A poly-crystalline p-type Ge film was grown initially at 360 °C for 3 min and then at 330 °C for another 30 min. The growth pressure was 28 Torr with flow rates of 10, 14 and 100 standard cubic centimeters per minute (sccm) for germane (GeH_4), diborane (B_2H_6 , 100 ppm in He) and hydrogen (H_2 , Semiconductor Grade), respectively. The film growth rate under these conditions was ~ 7.5 nm min⁻¹ for a total film thickness of ~ 250 nm. For n-type Ge film growth (Supplementary Fig. 5b) a 2.8 sccm PH_3 flow rate was used instead of B_2H_6 . For Cu patterning experiments, a 250 nm thick Cu film was deposited on p-type Si substrate by DC sputtering (Orion 3, AJA International, Inc.) at a pressure of 4 mTorr with 12 sccm of Ar and a gun process current and voltage of 1 A and 455 V, respectively. For Co patterning and catalyst studies, electron-beam evaporation was used to deposit a 300 nm thick Pt film on p-type Si substrate followed by a 250 nm film of Co.

For the 3D surface patterning in Fig. 1d, a Si <111> p-type substrate was patterned with $45 \mu\text{m} \times 45 \mu\text{m}$ regions using electron beam lithography through PMMA (400 $\mu\text{C cm}^{-2}$, 1.4 nA beam current). A 150 nm Cr film was deposited by thermal evaporation followed by acetone lift-off. A Si deep reactive ion etch (SF_6) was performed for 10 min in an inductively coupled plasma reactor (Surface Technology Systems ICP RIE, SPTS). A room temperature Cr etch was performed for 2 min in ceric ammonium nitrate (Cr etchant, Sigma Aldrich) to remove the Cr RIE mask. Thereafter, Ge CVD deposition was performed as described above.

After material (Ge or Cu) deposition, the substrate was coated with a 500 nm thick layer of S1805 photo-resist (S1805, MicroChem Corp.) or PMMA e-beam resist (PMMA C5, MicroChem Corp.). Using photolithography (5 s exposure) or electron beam lithography (400 $\mu\text{C cm}^{-2}$, 1.4 nA beam current), $80 \mu\text{m} \times 2 \mu\text{m}$ (length \times width) lines or $2 \mu\text{m} \times 2 \mu\text{m}$ dots were defined through the aforementioned resists to the underlying Ge film. A small region at the top of the substrate was left uncovered by resist in order to facilitate electrical contact via a Cu alligator clip to the potentiostat. The back and sides of the substrate were covered with a lacquer (Microshield, Tolber Chemical) to electrically passivate the substrate. For the cross-sectional sample characterized in Fig. 2a-d, a ~ 15 nm thick Au/Pd film was deposited to assist in clear differentiation of the patterned feature from the carbon film intentionally deposited to protect the sample during FIB milling.

Cyclic Voltammetry. A two-compartment (50 mL compartments separated by a glass frit of medium porosity) electrochemical cell was filled with 0.1 M sulfuric acid and the substrate (see Substrate Preparation) was submerged into one compartment. iR compensation was performed prior to every patterning experiment and yielded typical resistance values in the range of 500 – 1500 Ω . Standard three-electrode cyclic

voltammetry experiments were conducted using a Ag/AgCl reference electrode (BAS Inc.), a Pt mesh counter electrode, and potentiostat (760D series, CH Instruments Inc.). After concluding the cyclic voltammetry, the resists and lacquer were removed by soaking in acetone for ~1 min followed by a 10 s rinse in isopropanol. For Ge patterning, scans were initiated at the open circuit potential, which was 0.1 V. For the data shown in Supplementary Fig. 3, a 0.1 M sodium sulfate solution was used. All electrolytes were prepared from reagent grade chemicals and type I water (18 M Ω resistivity).

Catalyst Preparation and Characterization. The patterned cobalt was oxidized to the CoP_i catalyst at 0.95 V for 30 min in 0.1 M KPO₄ (pH 7.0), at which point steady-state was observed (Supplementary Fig. 6b). Faradaic efficiency was calculated using a fluorescent oxygen sensor (Ocean Optics) in a gas-tight electrochemical cell. The solution and headspace were purged with N₂ for an hour and the sensor was placed in the headspace. Electrolysis was performed at 1.0 V (vs. Ag/AgCl) in 0.1 M KPO₄ (pH 7.0) for 10 h.

SEM. SEMs were acquired using the SE2 detector on a Zeiss Supra55VP (Carl Zeiss AG) operating at 7 kV. The SEM images in Fig. 2e were false colored using the Copper Color Table in Igor Pro (WaveMetrics, Inc.) in order to aid in clear visualization of the rings.

EDS. Low-resolution EDS maps (Figs. 1d and 3c,d) were acquired on an SEM operating at 7 kV with 60 μ m aperture size and WD = 8.5 mm. EDS parameters included a dwell time of 200 ms and a frame resolution of 1024 \times 800. High-resolution EDS maps (Fig. 2d) were acquired on an aberration corrected STEM (Libra 200 MC, Carl Zeiss AG) operating at 200 kV with twin EDS detectors and drift correction. EDS parameters included a dwell time of 500 ms and a frame resolution of 1024 \times 800.

AFM. Topographic maps were acquired using an MFP-3D AFM (Asylum Research) with an Al coated Si AFM tip ($f \sim 300$ kHz, AC160TS). Data were acquired in AC mode at a 0.6 kHz scan rate. Using the Asylum software package, a 1st order Flatten procedure was applied to the raw data to correct for a mild distortion of the substrate plane. For the AFM maps in Fig. 1e, a N \times N median filter (size = 1) was applied as was the "Mocha" color table for the z-axis data (Asylum software).

TEM of cross-sections. The axial cross-section of a substrate patterned with rings was prepared by Ga⁺ focused ion-beam milling (Zeiss NVision 40, Carl Zeiss AG). To protect against subsequent FIB damage, the sample was first coated with a ~50 nm thick carbon film inside the FIB under SEM mode followed by ~550 nm of carbon under FIB mode. FIB milling was used to excise a wedge from the substrate and was followed by FIB welding of the wedge to a nano-manipulator needle with tungsten. The wedge was subsequently transferred and welded to a specialty Cu TEM grid. The section was reduced to a thickness of ~60 nm using FIB milling. Bright-field TEM images were acquired on a TEM operating at 200 kV (JEOL 2100, JEOL Ltd.).

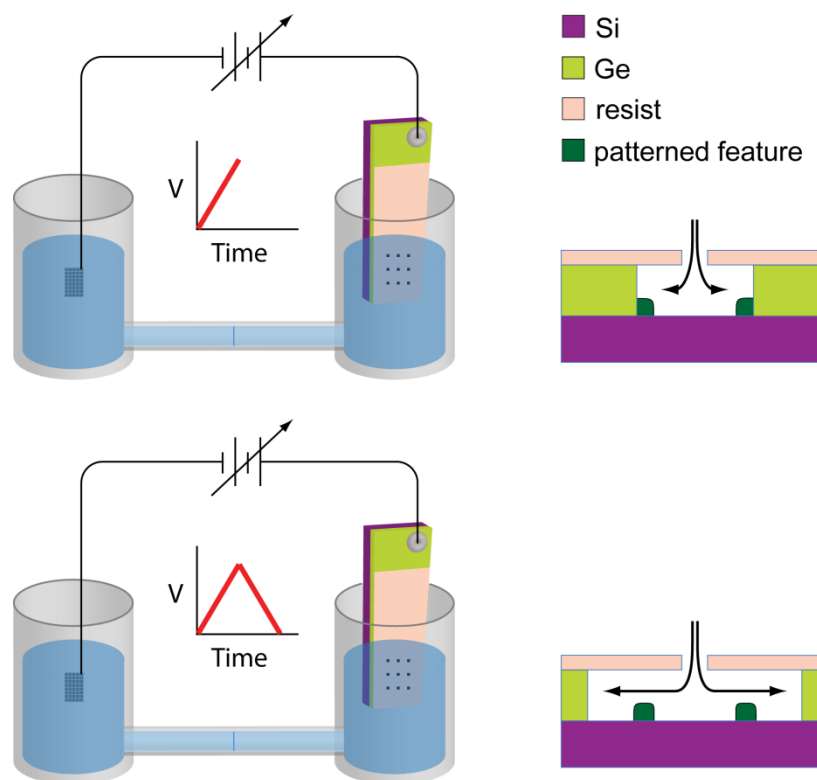


Figure S1 | Electrochemical set-up of RIPPLE technique. Top and Bottom: Schematics of the RIPPLE method showing a 2-compartment electrochemical cell with a Pt mesh electrode submerged in the left chamber and the working electrode, which undergoes patterning, submerged in the right chamber. The working electrode, whose axial cross-section is shown at right, consists, for example, of a Ge thin film (green) that is exposed at defined sites (e.g. dots) through a resist layer (beige). Top: Both electrodes are immersed in acidic solution (blue) and a linearly ramped potential sweep (thick red line) is applied (e.g. between 0.1 and 1.2 V vs. Ag/AgCl). Lateral etching of Ge proceeds underneath the resist layer. Bottom: A return potential sweep is applied leading to continued etching of Ge and site-selective formation of patterned features.

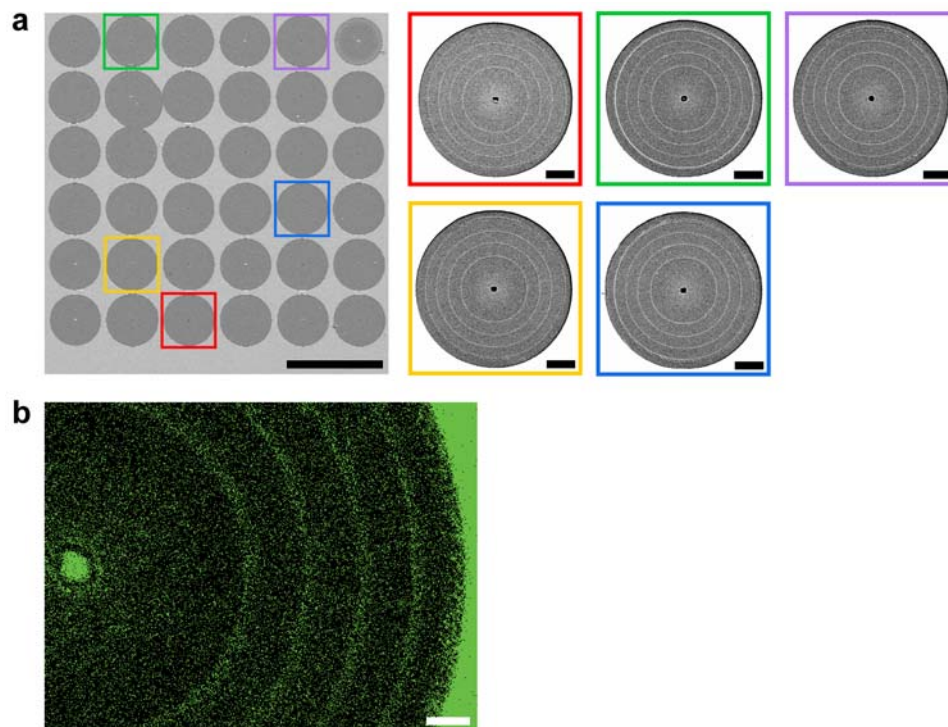


Figure S2 | Geometry and composition of patterned concentric rings. a, Left: SEM image of an array of 36 concentric rings; scale bar, 100 μm . Right: SEM image gallery of concentric ring patterns highlighted in image at left; scale bar, 10 μm . The concentric rings form well-defined, uniform circles. **b**, Planview EDS elemental map of Ge for a feature containing 4 rings; scale bar, 2 μm .

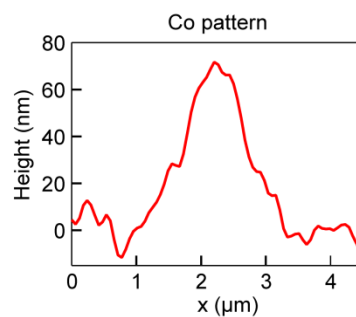
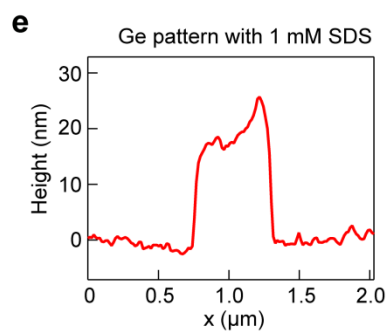
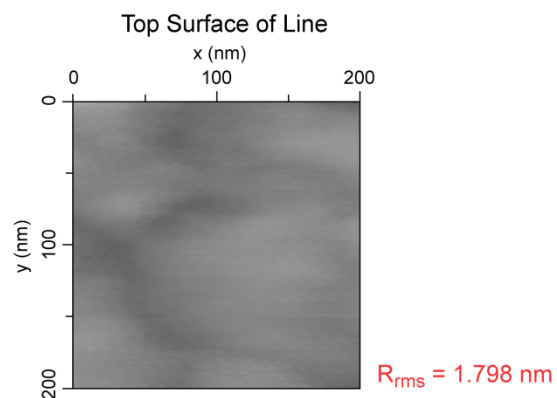
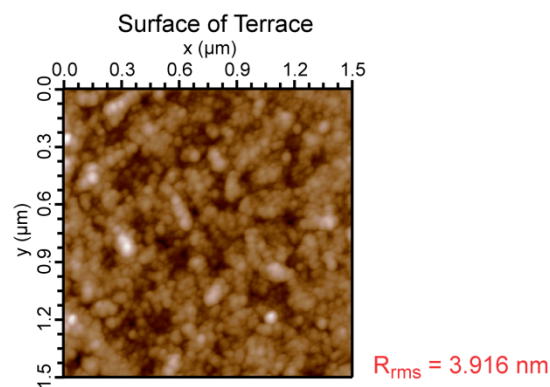
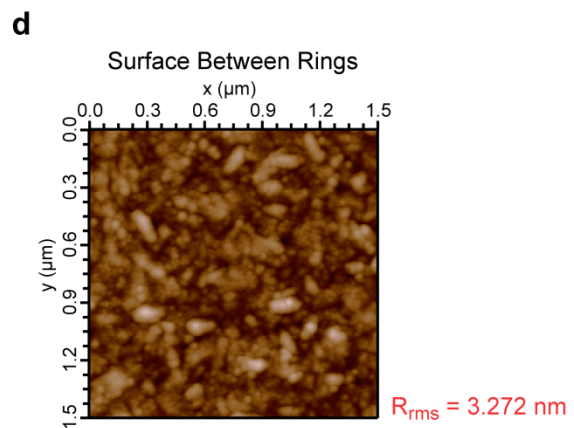
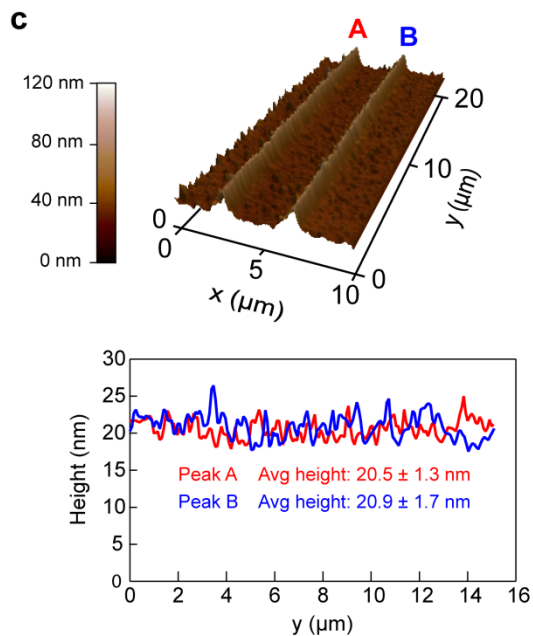
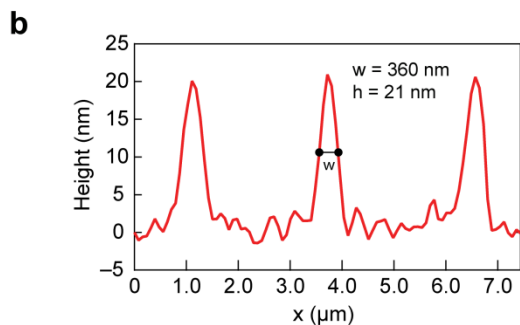
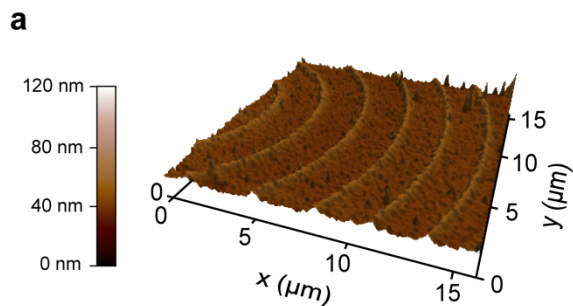


Figure S3 | Topographical analysis of patterned Ge rings by AFM. **a**, High-resolution AFM map showing topography of uniform patterned Ge rings on Si. **b**, Line-scan across 3 rings patterned on Si revealing a feature height and width of 21 nm and 360 nm, respectively. **c**, Top: High-resolution AFM map of parallel lines (cf. Fig. 1b). Bottom: Peak height across 15 μm stretch of the lines labeled 'A' and 'B' in AFM map above. Inset reveals an average height (20.5 nm and 20.9 nm) and standard deviation (1.3 nm and 1.7 nm) for both peaks that agrees well with measurements for rings. Overall, these data attest to the good uniformity of the features' size across the pattern. **d**, High-resolution AFMs of $1.5 \times 1.5 \mu\text{m}$ area of the substrate surface between patterned concentric Ge rings (top), of $1.5 \times 1.5 \mu\text{m}$ area of the surface of a terrace prepared as mentioned in Fig. 1e (middle), and of $200 \times 200 \text{ nm}$ area of the top of a single ring (bottom). Root mean squared roughness (R_{rms}) values calculated from raw height data are shown in red. **e**, Left: AFM line-scan across a Ge ring patterned under standard conditions with 1 mM sodium dodecyl sulfate in the 0.1 M sulfuric acid electrolyte. Right: AFM line-scan across a patterned Co ring (cf. Fig. 4). These data attest to the ability to adjust and improve the morphology of RIPPLE defined patterns.

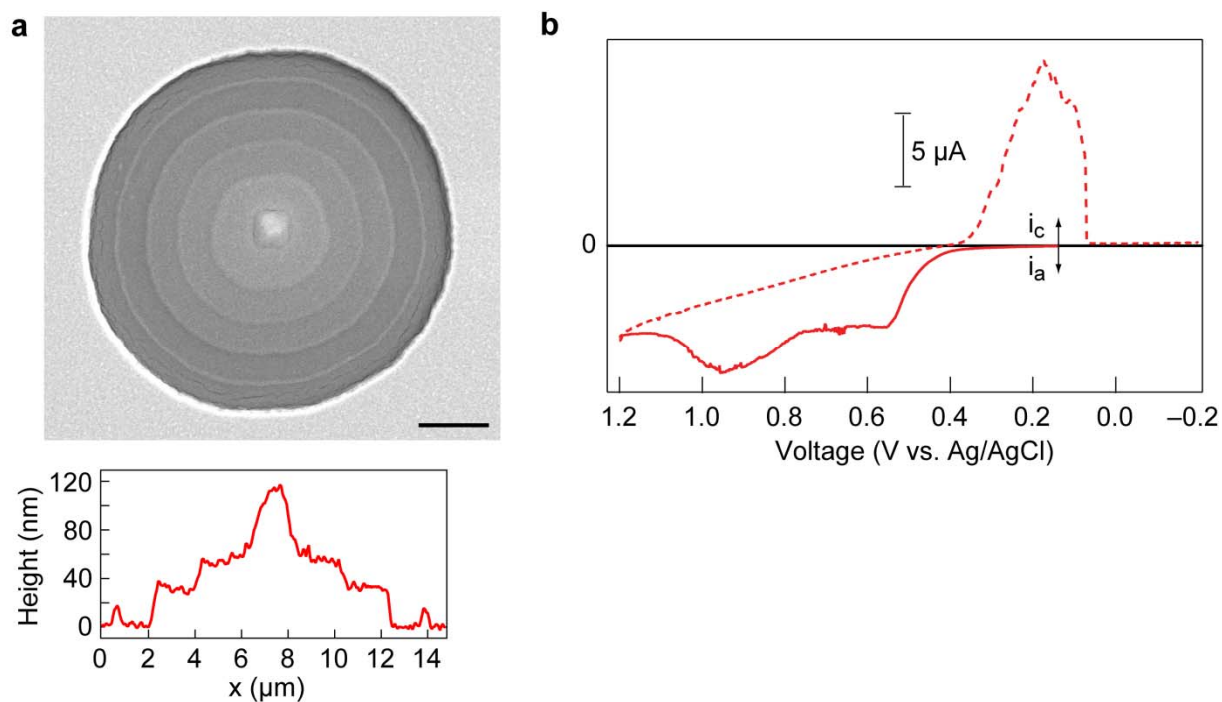


Figure S4 | Pattern morphology with CV performed in Na_2SO_4 . **a**, Top: SEM image of a patterned substrate after 5 CVs in 0.1 M Na_2SO_4 ; scale bar, 4 μm . Bottom: AFM line scan across the diameter of a pattern reveals a concentric terrace structure with height decreasing in discrete steps from the central pillar to the periphery of the pattern. **b**, 1 CV trace acquired in 0.1 M Na_2SO_4 distinguished by appearance of quasi-reversible waves consistent with the pattern formation by the material that is discernible in the SEM image.

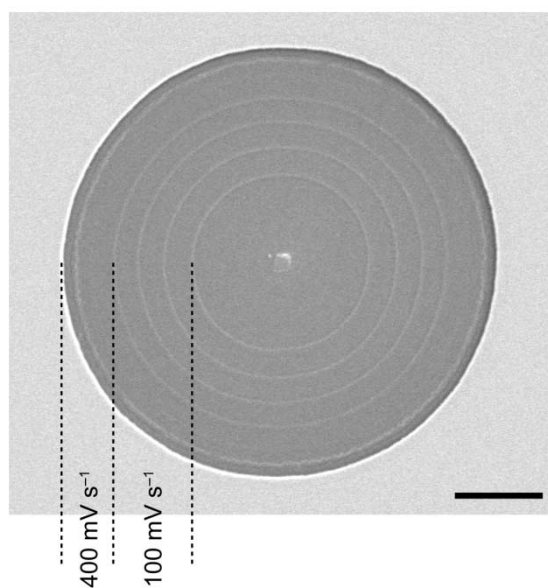


Figure S5 | Single patterning experiment at two scan rates. In a single uninterrupted experiment, an equal number of CVs was performed first at 100 mV s⁻¹ and then at 400 mV s⁻¹. The SEM image shows that the first set of patterned rings has an average period of 2.80 μm in good agreement with data (Fig. 3a) for rings patterned solely at 100 mV s⁻¹; scale bar, 10 μm . The rings patterned following the transition to a faster scan rate are less clearly defined.

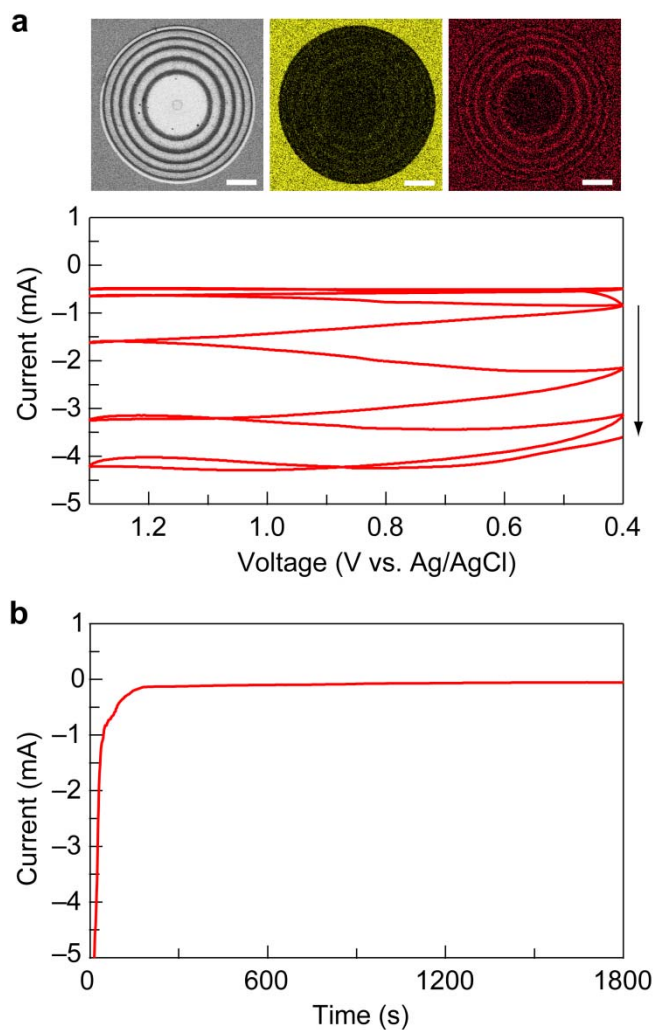


Figure S6 | Patterning and anodization of Co. **a**, Top: SEM of patterned Co (left), Co EDS map (middle), and O EDS map (right); scale bar, 10 μm . Bottom: Cyclic voltammogram in 0.1 M H_2SO_4 of a 250 nm metallic Co film (see Methods). Arrow denotes beginning of first scan and the direction of progression of subsequent scans. Scan rate during patterning was 200 mV s^{-1} . **b**, Anodization of patterned Co at a potential of 0.95 V vs. Ag/AgCl (without iR compensation) for 30 min in 0.1 M KPO_4 , pH 7.0 electrolyte.

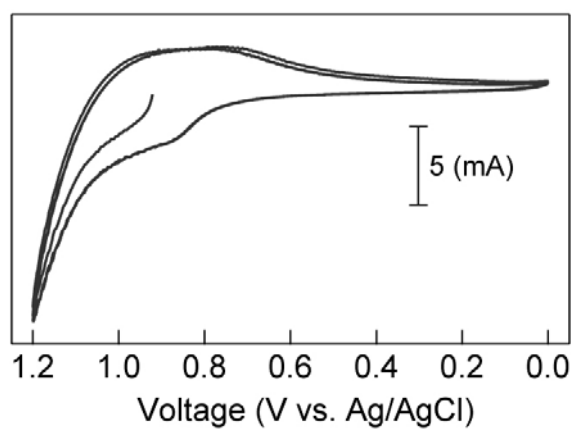


Figure S7 | CVs of patterned CoP_i. Cyclic voltammograms of patterned CoP_i catalyst at 100 mV s⁻¹ in 0.1 M KP_i (pH 7) electrolyte. The catalytic wave initiates at ~0.9 V.

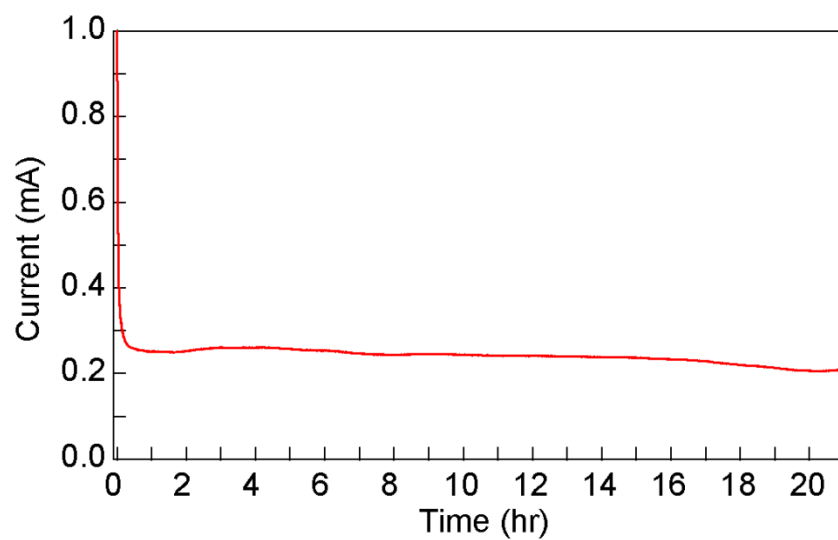


Figure S8 | Stability of patterned CoP_i catalyst. Current passed over 21 hr of electrolysis performed on a patterned CoP_i catalyst at 1.0 V (vs. Ag/AgCl) in 0.1 M KP_i (pH 7.0). The transient at very early times is due to double-layer charging.